Analytical and Bioanalytical Chemistry (2021) 413:1827–1836
https://doi.org/10.1007/s00216-020-03150-1

RESEARCH PAPER

Electrochemical detection of alkaline phosphatase activity through enzyme-catalyzed reaction using aminoferrocene as an electroactive probe

Wenbin Wang[1] · Jing Lu[2] · Lulu Hao[2] · Huaixia Yang[2] · Xuejie Song[1] · Fuchun Si[1]

Received: 28 October 2020 / Revised: 5 December 2020 / Accepted: 23 December 2020 / Published online: 22 January 2021

Abstract

As a nonspecific phosphomonoesterase, alkaline phosphatase (ALP) plays a pivotal role in tissue mineralization and osteogenesis which is an important biomarker for the clinical diagnosis of bone and hepatobiliary diseases. Herein, we described a novel electrochemical method that used aminoferrocene (AFC) as an electroactive probe for the ALP activity detection. In the condition with imidazole and N-(3-dimethylaminopropyl)-N′-ethylcarbodiimide hydrochloride (EDC), the AFC probe could be directly labeled on single-stranded DNA (ssDNA) by one-step conjugation. Specifically, thiolated ssDNA at 3′-terminals was modified to the electrode surface through Au–S bond. In the condition without ALP, AFC could be labeled on ssDNA by conjugating with phosphate groups. In the presence of ALP, phosphate groups were catalyzed to be removed from the 5′-terminal of ssDNA. The AFC probe cannot be labeled on ssDNA. Thus, the electrochemical detection of ALP activity was achieved. Under optimal conditions, the strategy presented a good linear relationship between current intensity and ALP concentration in the range of 20 to 100 mU/mL with the limit of detection (LOD) of 1.48 mU/mL. More importantly, the approach rendered high selectivity and satisfactory applicability for ALP activity detection. In addition, this method has merits of ease of operation, low cost, and environmental friendliness. Thus, this strategy presents great potential for ALP activity detection in practical applications.

Keywords Alkaline phosphatase · Biosensor · Electrochemical · Enzyme-catalyzed reaction · Aminoferrocene

Introduction

Chronic kidney disease (CKD) is a global public health problem [1]. According to the statistics of chronic kidney disease collaboration, the number of patients with CKD worldwide reached 9.1% in 2017 [2]. Due to the existence of cardiovascular complications, CKD always has high incidence of morbidity and mortality [3]. The main manifestation of cardiovascular events is vascular calcification caused by mineral metabolism disorders [4]. More importantly, ALP plays a vital role in tissue mineralization and osteogenesis [5]. ALP is a dimeric metalloprotein with molecular weight of 70 to 180 kDa, containing Zn^{2+} and Mg^{2+} [6, 7]. As an important hydrolytic enzyme, ALP catalyzes the removal of the phosphate groups from nucleic acids, proteins, and small molecules under alkaline conditions [8]. ALP widely exists in biological tissues such as liver, bone, intestines, kidney, and placenta [9]. In addition, the abnormality of ALP activity has been found to be closely associated with various diseases, including liver dysfunction, bone injury, breast and prostatic cancer, diabetes, Wilson's disease, and hematological disease [10]. Therefore, the detection of ALP activity and screening of inhibitors are crucial for the diagnosis and treatment of ALP-related diseases.

In recent years, various strategies have been reported for the detection of ALP activity, such as fluorometry, colorimetry, chemiluminescence method, electrochemical method, isotope labeling, and surface-enhanced Raman scattering method [11–16]. Among these methods, fluorimetry and colorimetric have drawn special attention due to their fast response, and

✉ Huaixia Yang
yanghuaixia886@163.com

✉ Xuejie Song
sxj2019@126.com

✉ Fuchun Si
sifc2000@hotmail.com

[1] Academy of Chinese Medical Sciences, Henan University of Chinese Medicine, Zhengzhou 450046, China

[2] Pharmacy College, Henan University of Chinese Medicine, Zhengzhou 450046, China

convenience. Unfortunately, these detection methods are still not practical enough owing to limited linear range and poor selectivity. Compared with other methods, electrochemical biosensor has drawn considerable attention due to its attractive advantages of quick response, simplicity, easy portability, and low cost [17]. For example, Miao and his co-workers utilized hexaammineruthenium (III) chloride as the electroactive substance; two complementary DNA fragments and exonuclease were used to assay the activity of ALP [18]. Lee's group reported a strategy for ALP activity detection by electrochemical impedance spectroscopy (EIS) [19]. The complex of pyrophosphate (PPi) and Cu^{2+} was employed as the substrate of ALP, the released Cu^{2+} could undergo a redox reaction with ascorbic acid (AA), and the oxidation products accumulated which blocked the electron transfer on the electrode surface, which led to the increase of resistance. Although these two schemes are relatively easy to operate, they suffer from the unsatisfactory sensitivity and selectivity. Despite that progress has been made in the electrochemical detection of ALP activity, relatively little advance has been made in the construction of an electrochemical biosensor with simple operation, time saving, labor saving, low cost, and satisfactory analytical performance.

Generally speaking, quantitative analysis of biomolecules could be effectively and conveniently reached through monitoring the proportionally labeled electroactive probes. Up to now, ferrocene derivatives have become the most commonly used electroactive probes in electrochemical biosensor territory owing to favorable redox properties. Several available strategies that exploited ferrocene derivatives as electroactive substances have been proposed. For example, ferrocene derivatives were modified to the end of molecular beacons [20]; versatile coupling linkers were used to label target ssDNA with ferrocene derivatives before/after hybridization [21], using "Click" chemistry to connect acetylene ferrocene to azide-modified DNA [22]. However, it is time consuming and complicated to prepare, separate, and purify the labeled DNA and catalyst CuAAC for "Click" chemistry is toxic. Hu's group reported an electrochemical DNA biosensor strategy using AFC as electroactive probe [23]. As cross-linking mediums, EDC can effectively activate the phosphate group at the end of ssDNA to form active intermediates, which can be replaced by AFC. Thus, the AFC probe could be directly linked to the ssDNA through one-step conjugation with phosphate group in the condition with imidazole and EDC. The simplicity of this strategy gives it great potential in the microarray areas.

Inspired by above opinion, we described a novel strategy of combining conjugation of AFC to phosphate groups and dephosphorylation of ALP to achieve ALP activity detection. The assay of ALP activity involves the following: (1) the thiolated ssDNA at 3′-terminals was self-assembled onto the surface of the Au electrode via S–Au bond; (2) after cultivated by ALP, part of 5′-terminal phosphate group was removed from DNA on the electrode surface; (3) in the presence of EDC and imidazole, AFC was used as an electroactive probe to label ssDNA which contains phosphate group. Compared with the condition without ALP, the electrochemical signal was decreased because of the decrease of labeled AFC on the Au surface. Under optimal conditions, the biosensor has a good linear response in the range of 20 to 100 mU/mL with the LOD of 1.48 mU/mL, and it renders satisfactory selectivity and interference resistance in serum samples. In addition, this strategy has merits of ease of operation, low cost, and environmental friendliness. Thus, this strategy presents great potential for ALP activity detection in practical applications.

Material and methods

Materials and reagents

The ssDNA with sequence 3′-HS-$(CH_2)_6$-GTG TGT GTG TGT GTG TGT GT-HPO^{4-}-5′ was custom-made by Sangon Biotech (Shanghai, China). 6-Mercapto-1-hexanol (MCH) was obtained from Sigma-Aldrich (St. Louis, USA). ALP, Tris–EDTA buffer (TE buffer, pH = 8.0), Tris, EDC, imidazole, glucose oxidase (GOx), pepsin, and bovine serum albumin (BSA) were all purchased from Beijing Solarbio Science & Technology Co., Ltd (Beijing, China). AFC was obtained from Shanghai yuanye Bio-Technology Co., Ltd (Shanghai, China). Human serum sample was obtained from Yu Duo Co., Ltd. (Shanghai, China). All other reagents were of analytical purity. The ultrapure water in all experiments was gained from a Millipore water purification system (≥ 18.25 MΩ cm).

Tris buffer (containing 0.1 M Tris–HCl, 2 mM $MgCl_2$, 0.2 mM $ZnCl_2$, pH = 8.0) was prepared and utilized as ALP stock and wash solution, and various concentrations of ALP solutions were prepared by serial dilution. 0.1 M imidazole solution was prepared by ethanol solution, and adjusted its pH with hydrochloric acid. These ssDNA, MCH, Tris–HCl, $MgCl_2$, $ZnCl_2$, and KNO_3 solutions were prepared with TE buffer, 70% ethanol, H_2O, H_2O, H_2O, and H_2O respectively.

Apparatus

The differential pulse voltammetry (DPV), cyclic voltammetry (CV), and EIS tests were performed at normal temperature (25 °C) with a three-electrode system, which composed of Au electrode (diameter = 2 mm), platinum wire electrode, and saturated calomel electrode as work electrode, counter electrode, and reference electrode, respectively. EIS measurements were tested in 0.1 M KNO_3 solution (containing 5 mM $[Fe(CN)_6]^{4-/3-}$) (equimolar) and performed on Autolab PGSTAT204 (Eco Chemie, Netherlands). CV and DPV were conducted on a CHI 760E electrochemical

workstation (Shanghai CH Instruments Inc, China). The measurement of static water contact angle (WCA) was made by droplet shape analyzer-DSA100 (KRÜSS, Germany).

Fabrication of biosensor

Prior to decoration, bare Au electrode was first polished to a mirror-like surface with 0.3 and 0.05 μm Al_2O_3 slurry. Next, the electrode was successively rinsed ultrasonically for 2 min with absolute ethanol and ultrapure water. Afterwards, it was chemically cleaned in newly prepared piranha solution (98% concentrated sulfuric acid and 30% hydrogen peroxide, 3:1 v/v) for 15 min and rinsed with water. Then, the gold electrode was electrochemically cleaned by CV in freshly prepared 0.5 M H_2SO_4 solution (scan rate: 0.1 V/s, potential range: −0.3~1.5 V) until stable curves were achieved. Finally, it was ultrasonically rinsed with ultrapure water and dried with nitrogen stream.

Ten microliters of ssDNA (1 μM) was dropped onto the Au electrode surface and incubated at 37 °C for 1.5 h, and then washed with TE buffer and ultrapure water to remove the excess ssDNA. The ssDNA-modified electrode was soaked in 400 μL of MCH (2 mM) solution so that the nonspecific binding sites on the Au electrode surface were blocked. After rinsing with 70% EtOH and ultrapure water, reaction was performed in 10 μL of Tris buffer (pH = 8.0) that contains ALP (50 mU/mL) at 37 °C; then, the electrode was rinsed with Tris–HCl buffer and water respectively. Afterwards, 10 μL of mixed solution of EDC and AFC which freshly dissolved in 0.1 M imidazole solution was added onto the electrode surface and the concentration of EDC was maintained at 10 mg/mL incubated at 25 °C to label electroactive probes, then rinsed with 80% EtOH solution and ultrapure water to remove the unreacted substance. Finally, the electrode was immersed in 10 mL KNO_3 (1.0 M) solution to obtain the oxidation current of AFC via DPV and the potential range was 0 to 0.5 V.

Results and discussion

Principle of this biosensor for ALP detection

In this work, the thiol-containing ssDNA was fixed onto the Au electrode surface via Au–S bond self-assembly. EDC and imidazole acted as a synergistic cross-linking medium to make the amino group in AFC form a phosphate bond with the phosphate group on the DNA fragment. In the presence of imidazole, the water-soluble carbodiimide EDC rapidly activated the free phosphate group at the 5′-terminals of ssDNA to generate a phosphoryl imidazoline intermediate, which had a high reactivity with amine-containing nucleophiles [24]. The schematic diagram of ssDNA labeled by AFC is illustrated in Fig. 1. Zn^{2+} and Mg^{2+} played vital role in the catalytic activity of ALP and the conformational stability of the active site. Under the catalysis of Zn^{2+} and Mg^{2+}, ALP could remove the phosphate group from DNA molecules and generated phosphate ions and free hydroxyl groups by hydrolyzing phosphate monoesters [25]. The ssDNA without the phosphate group cannot be labeled with the AFC electroactive probe, which resulted in a drop in the electrochemical detection signal. The principle of ALP detection is illustrated in Scheme 1.

Feasibility of electrochemical biosensor for ALP detection

To confirm the feasibility and effectivity of the fabricated biosensor toward the detection of ALP activity, DPV was applied to detect the currents of different modified electrodes. As illustrated in Fig. 2A, no obvious oxidation current could be observed in the absence of ssDNA (curves c) and AFC (curves d) (except for a weak background signal). Compared with the condition without ALP (curves a), a weak oxidation peak was detected at the potential around 0.25 V after cultivated by ALP (curves b), corresponding to the oxidation of AFC probe. This indicated that the AFC tags failed to label the ssDNA because the ALP had catalyzed the removal part of the free phosphate groups of the ssDNA. These results clearly demonstrated the feasibility of this strategy for ALP activity detection.

CV was utilized to characterize the AFC probes that labeled on the electrode surface in 1.0 M KNO_3; the scan rates were from 10 to 200 mV/s and the potential was from 0 to 0.6 V. As shown in Fig. 2B, the redox currents and scan rates presented a good linear relationship, which confirmed that the redox process was not dependent on diffusion [26], and indicated that AFC was tethered to the Au electrode surface via covalent bond [27].

Characterizations

EIS was employed to characterize the preparation process of this biosensor, because EIS had a high sensitivity to examine the microscopic interfacial variation of the electrode surface. As shown in Fig. 2C, the charge transfer resistance (R_{ct}) is equal to the diameter of semicircle in Nyquist plots [28]. The semicircle of the bare Au electrode was the smallest, which was observed in the impedance spectrum (~ 244 Ω, curve a). After modification of ssDNA, the R_{ct} increased owing to the poor electron transfer ability of the monolayer (~ 321 Ω, curve b) [29]. Subsequently, MCH was used to occupy the unbound sites on the electrode surface, which led to a further increase in resistance (~ 476 Ω, curve c). After cultured by ALP, the R_{ct} was decreased; this might be mainly due to the negatively charged phosphate in ssDNA which was

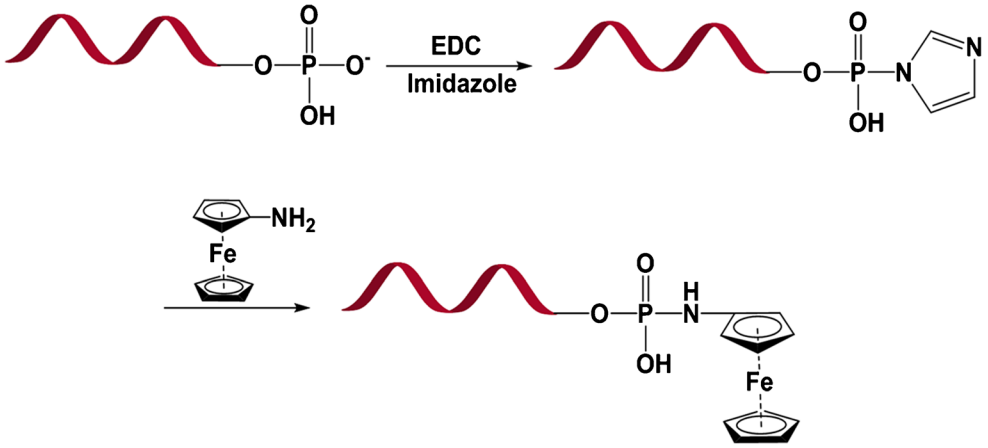

Fig. 1 AFC covalently labeled ssDNA in the presence of EDC and imidazole

hydrolysised removed by ALP [30], which promoted the electron transfer (~408 Ω, curve d). Finally, after modified by AFC, a further enhancement of R_{ct} owing to the steric effect of the labeled AFC probes (~546 Ω, curve e). These results indicated that the biosensor was fabricated successfully.

Moreover, the surface features of the modified electrode at each immobilization step were also investigated by CV. As can be seen from Fig. 2D, when ssDNA was modified on the bare Au electrode, the peak current decreased compared with the bare gold electrode (55.6~53.8 μA, curve a~b). Then, MCH was modified on the electrode surface by self-assembly, which caused a further decline of the peak current (51.2 μA, curve c). Curve d shows that the peak current was increased after cultivated by ALP (52.1 μA). Finally, the current was significantly decreased while AFC was attached to the electrode (48.9 μA, curve e). Therefore, the results of CV were consistent with EIS. All of these demonstrated that the construction process of this biosensor was effective.

The WCA is an effective method that characterizes the change of groups on the surface of materials [31]. Figure 3 shows the angle of the WCA at each step of the preparation process. It could be observed from Fig. 3a that the WCA of the bare Au electrode surface was 94.2° due to its hydrophobicity. After the ssDNA was modified onto the electrode, the WCA decreased to 82.3° owing to ssDNA which contains numerous hydrophilic groups (Fig. 3b). The WAC increased to 83.2° after MCH was modified on the electrode surface by self-assembly, which may be because MCH contains both hydrophilic hydroxyl groups and hydrophobic carbon chains so that the WCA does not change obviously (Fig. 3c). After

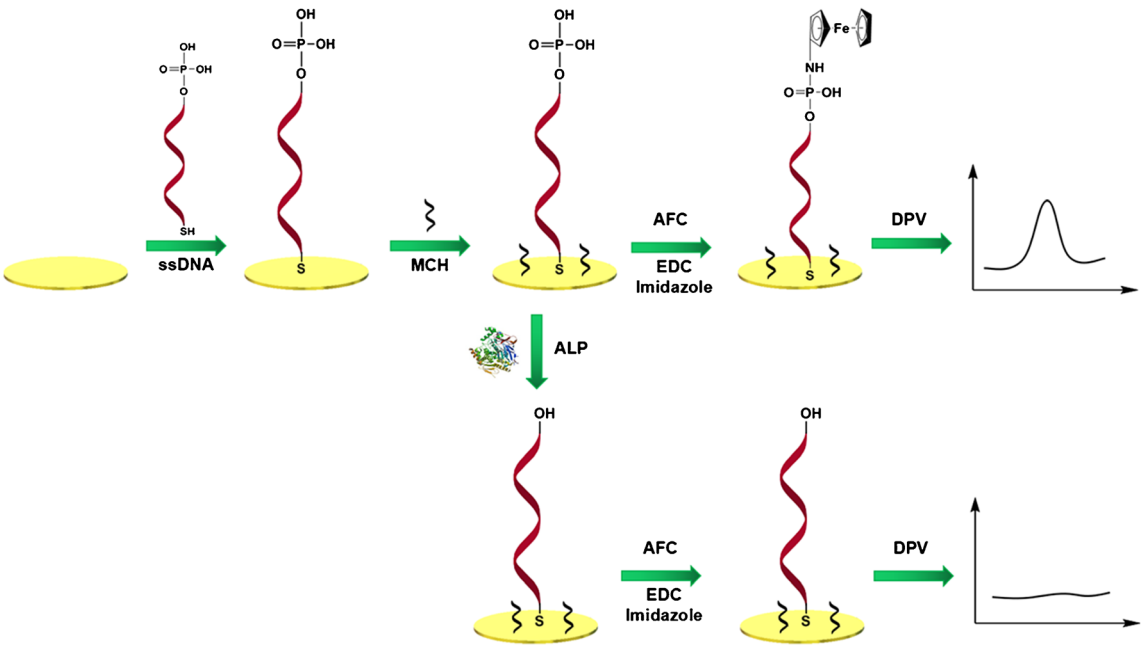

Scheme 1 Schematic illustration of electrochemical assay of ALP activity based on enzyme-catalyzed reaction

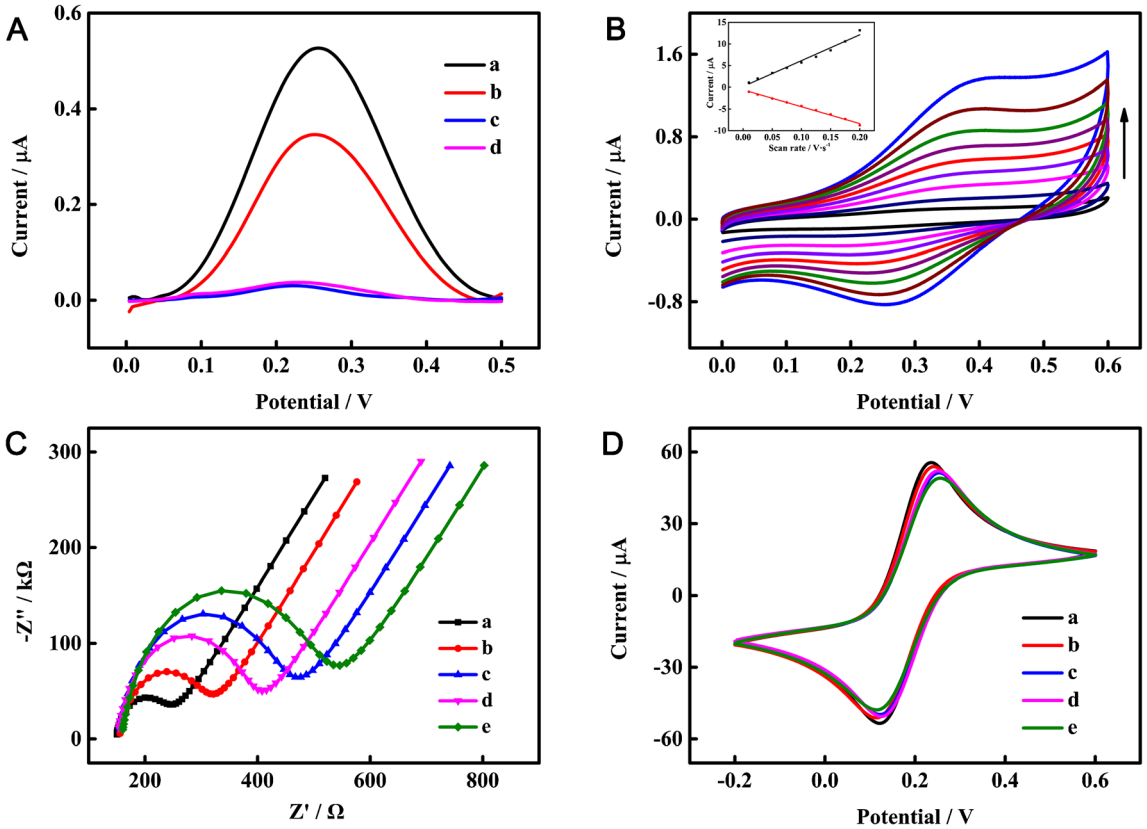

Fig. 2 (A) DPV curves of AFC/ALP/MCH/ssDNA/Au (b) in the condition without ALP (a), ssDNA (c), and AFC (d). (B) CV curves of AFC/ALP/MCH/ssDNA/Au at scan rates from 10 to 200 mV/s. (Inset) The correlation of reduction (red line) and oxidation (black line) peak current with the different scan rates. (C) EIS and (D) CV curves of Au (a), Au/ssDNA (b), Au/ssDNA/MCH (c), Au/ssDNA/MCH/ALP (d), and Au/ssDNA/MCH/ALP/AFC (e). The concentrations of ALP were all 50 mU/mL

cultivated by ALP, the change of WCA was not obvious; the WCA increased to 84.7° slightly owing to both phosphate and hydroxyl which are hydrophilic groups (Fig. 3d). Finally, the WCA was significantly increased while AFC was attached to the electrode surface because of the hydrophobicity of the ferrocene groups (Fig. 3e). Above all proved the feasibility of this electrochemical biosensor strategy.

Optimal conditions for the biosensor

To improve the sensitivity and efficiency, important experimental parameters were investigated so as to achieve the best analytical performance of the electrochemical biosensor.

Obviously, the ALP cultivation time is a significant prerequisite that leads to an alteration to the amount of free phosphate on the electrode surface. That is, the longer the reaction time is, the more the phosphate groups on 5′-terminal DNA are hydrolyzed and removed, which directly affects the number of AFC-labeled probes and leads to the reduction of oxidation current intensity. Figure 4a shows variation between ALP cultivation time and the oxidation current intensity. In the first 45 min, the current intensity decreased rapidly with the reaction time. After that, it decreased slowly until reached equilibrium at 60 min. Therefore, 60 min was the appropriate time of ALP cultivation in this strategy.

The analytical performance of this biosensor largely depends on the number of electroactive probes labeled on the ssDNA, which in turn is affected by the labeling time. In order to optimize the sensitivity of the biosensors, the influence of labeling time on the current signal was studied here. The current signal gradually increased before 105 min; then, it reached equilibrium which is observed in Fig. 4b. With the further increase of label time, the current intensity could not increase significantly. Consequently, 120 min was chosen as optimal time of labeled AFC probe.

The concentration of AFC also significantly affects the number of labeled AFC probes. In order to improve the analytical performance and achieve the maximum detection range of electrochemical biosensor for ALP detection, herein, the AFC probe concentration optimization of the sensor in the condition without ALP was studied. It could be seen from Fig. 4c that with the increase of AFC concentration, the current intensity gradually increased until it reached a stable value at 1.6 mg/mL. Compared with the sensor in the absence of

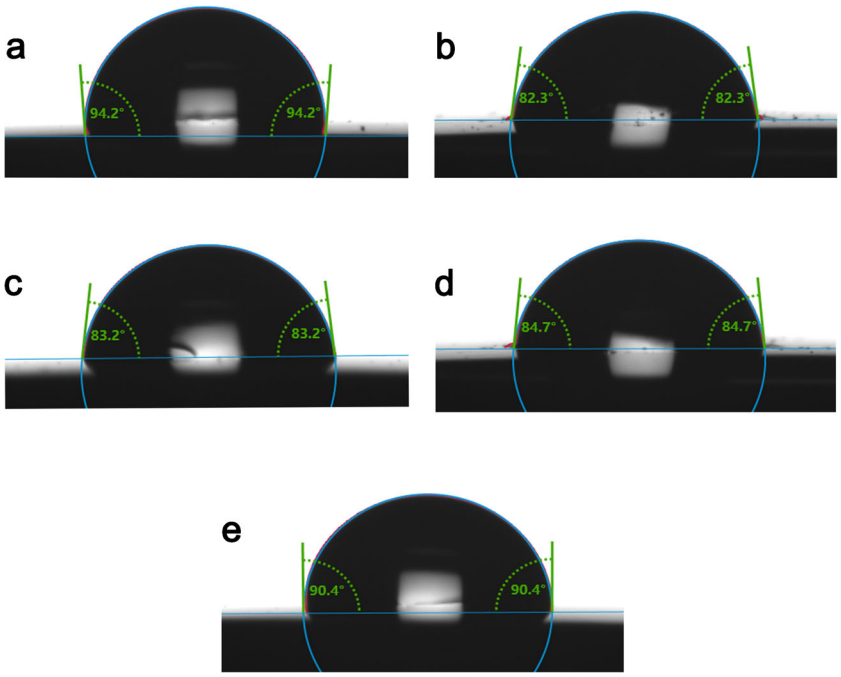

Fig. 3 Water droplet on the (a) Au, (b) Au/ssDNA, (c) Au/ssDNA/MCH, (d) Au/ssDNA/MCH/ALP, and (e) Au/ssDNA/MCH/ALP/AFC

ALP, the phosphate group on the surface of sensor cultivated by ALP is relatively less. Therefore, AFC labeled on the surface of the sensor cultivated by ALP could also reach saturation while the concentration of AFC is 1.6 mg/mL. Therefore, the optimal concentration of AFC was selected as 1.6 mg/mL in the subsequent experiments.

In addition, the effect of ssDNA concentration on electrochemical signal was studied in the absence of ALP. It could be seen from Fig. 4d that when the concentration of ssDNA was less than 0.5 μM, the electrochemical signal increased rapidly with the increase of the ssDNA concentration. There was no obvious change of electrochemical signal when the

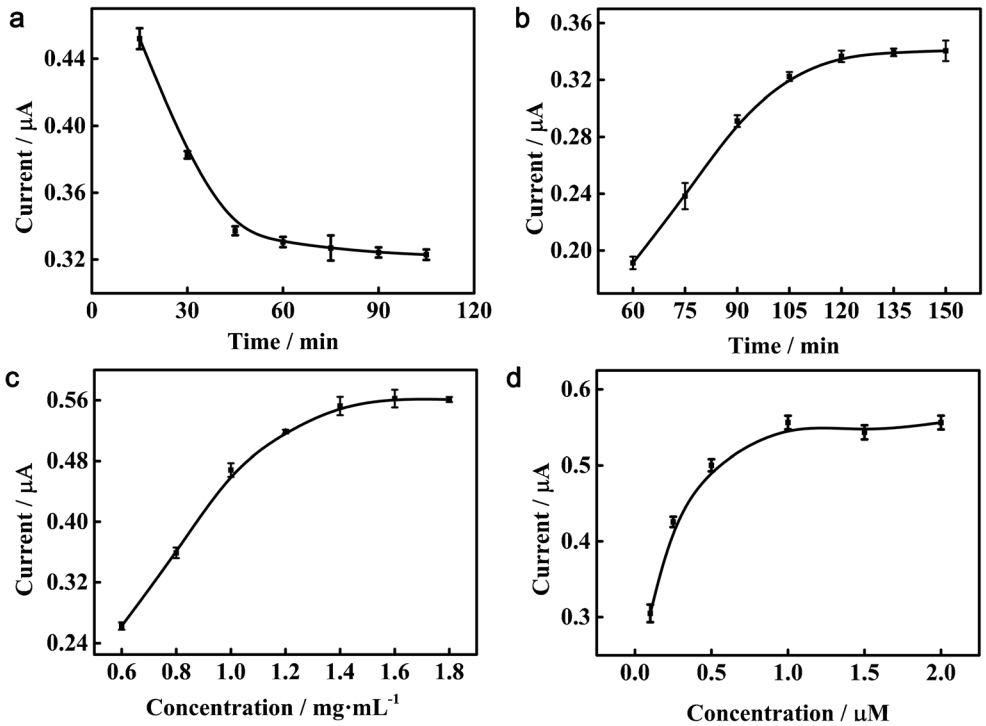

Fig. 4 The optimizations of (a) ALP incubation time. (b) AFC labeling time. (c) AFC concentration. (d) ssDNA concentration. The concentrations of ALP were all 50 mU/mL. Error bars = SD, $n = 3$

Table 1 Comparison with other methods for ALP activity detection

Method	Linear range (mU/mL)	LOD (mU/mL)	Refs
Fluorometry	25~200	10	[32]
Fluorometry	50~200	3.8	[33]
Colorimetric	100~600	10	[34]
Chemiluminescence	2~25	2	[35]
Electrochemistry	5~640	5	[36]
Electrochemistry	1000~20,000	100	[18]
Electrochemistry	20~100	1.48	This work

concentration was higher than 1 μM, which was because the amount of ssDNA modification on the electrode surface reached saturation. The above result showed that the optimal concentration of ssDNA was 1 μM.

Analytical performance

Under optimized conditions, the detection range and the LOD of this strategy for ALP activity detection were studied with different ALP concentrations. A good linearity was presented between current intensities and ALP activity concentrations from 20 to 100 mU/mL which is observed in Fig. 5. The corresponding regression equation was I (μA) = 0.55771 − 0.00381 [C_{ALP}/mU mL^{-1}] (R^2 = 0.9987), and LOD was 1.48 mU/mL (S/N = 3). As shown in Table 1, by comparing analytical performance with the proposed ALP activity detection and those reported previously, LOD of the established sensor was lower than that of many other methods.

Inhibition rate experiment

The inhibition rate of different concentrations of Na_3VO_4 on ALP activity was studied due to the inhibition rate of ALP which was closely related to drug screening and disease treatment. As depicted in Fig. 6a current intensities of this sensor gradually increased with the concentrations of Na_3VO_4, which indicated that Na_3VO_4 could inhibit ALP activity in a concentration-dependent manner. The diversification between inhibition rate of ALP activity and the concentrations of Na_3VO_4 is observed in Fig. 6b, and the IC_{50} value (the concentration of inhibitor when the ALP activity is inhibited by 50%) was estimated to be 2.35 mM. The above results demonstrate the effectiveness of this strategy in the clinical screening of ALP inhibitors.

Selectivity and anti-interference ability analysis

In order to validate the specificity in complex biological samples, the selectivity of the electrochemical biosensor approach was demonstrated by using GOx, pepsin, and BSA under the same experimental conditions. The concentrations of the ALP, pepsin, and GOx were all 50 mU/mL and the BSA was 100 μM. As could be seen from Fig. 7a, other enzymes and protein induced negligible change in the electrochemical signal. Because ALP had the special property of catalyzing the removal of the phosphate groups from ssDNA, the oxidation

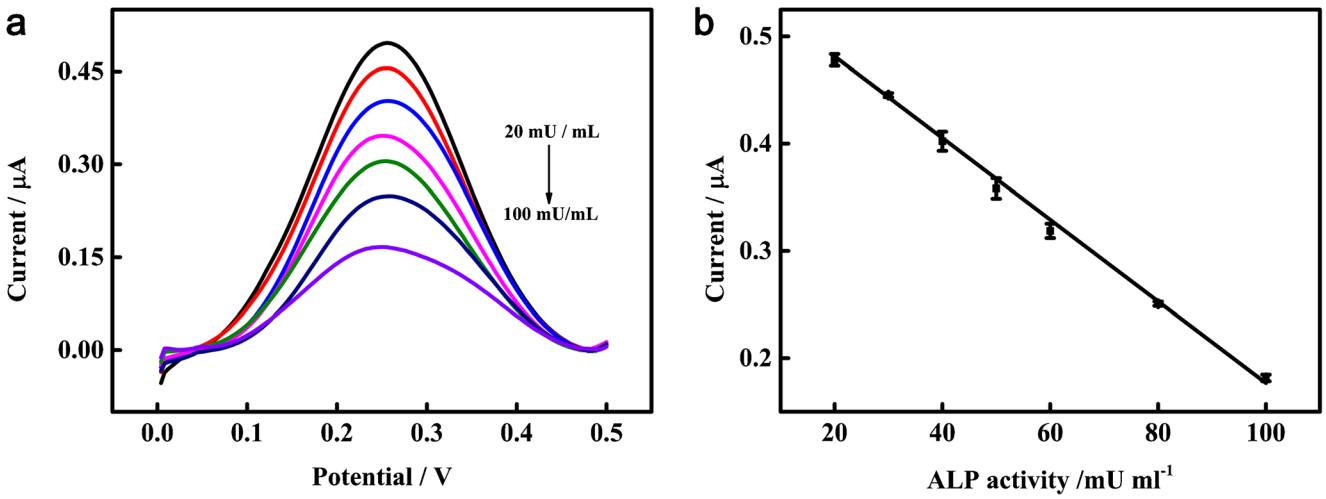

Fig. 5 (a) DPV curves of different concentrations of ALP. (b) Linear relationship curve between current signal and different ALP concentrations. The concentrations of ALP were 20, 30, 40, 50, 60, 80, and 100 mU/mL respectively. Error bars = SD, n = 3

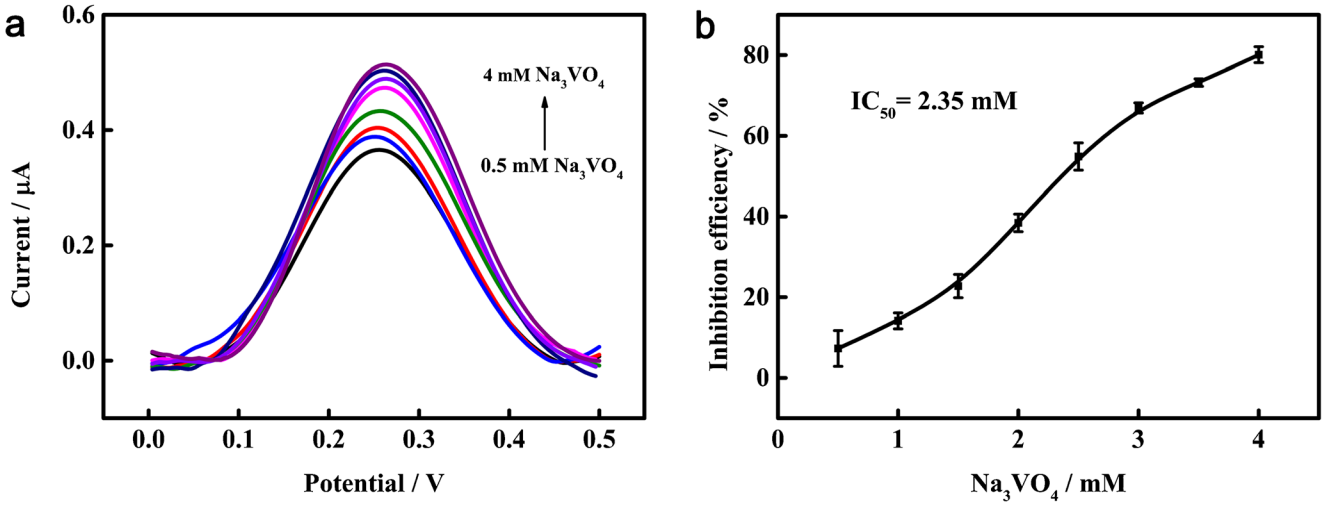

Fig. 6 (a) DPV curves of the mixed solutions of ALP and different concentrations of Na_3VO_4. (b) Correlation curve between inhibition rate of ALP activity and different Na_3VO_4 concentrations. The concentrations of ALP were all 50 mU/mL. The concentrations of Na_3VO_4 were 0.5, 1, 1.5, 2, 2.5, 3, 3.5, and 4 mM respectively. Error bars = SD, $n = 3$

peak current of the sensor cultivated by ALP could be significantly reduced. These results indicate that the strategy has high selectivity for ALP activity detection.

We investigated the current signal of ALP in 5% and 10% human serum samples so as to assess the anti-interference capability of the electrochemical biosensor approach. ALP of 50 mU/mL was prepared with 5% and 10% human serum samples respectively. The corresponding electrochemical signal of ALP in human serum sample was in comparison with the electrochemical signal in Tris–HCl buffer. As shown in Fig. 7b, compared with Tris–HCl buffer (b), the current signal of the 5% (c) and 10% (d) human serum increased by 2.86% and 7.62% respectively. Consequently, the strategy has satisfactory anti-interference capability in serum samples and presented certain potential in significant clinical applications.

Reproducibility and stability analysis

The inter-assays and intra-assays ($n = 5$) were performed to investigate the reproducibility of this electrochemical biosensor. In the condition with ALP, the relative standard deviation of the inter-assays and intra-assays was 5.5% and 4.6%, respectively. And in the absence of ALP, it was 2.2% and 3.6% for intra-assay and inter-assay, respectively. These results suggested that this electrochemical biosensor had satisfied reproducibility. In order to evaluate the stability of this strategy, long-term storage experiment was carried out. Five identically modified electrodes were freshly prepared and stored in 4 °C for 14 days. Compared with the freshly prepared electrodes, the current signal of those electrodes retained up to 92.7%. Thus, this electrochemical biosensor strategy presented satisfactory stability during storage.

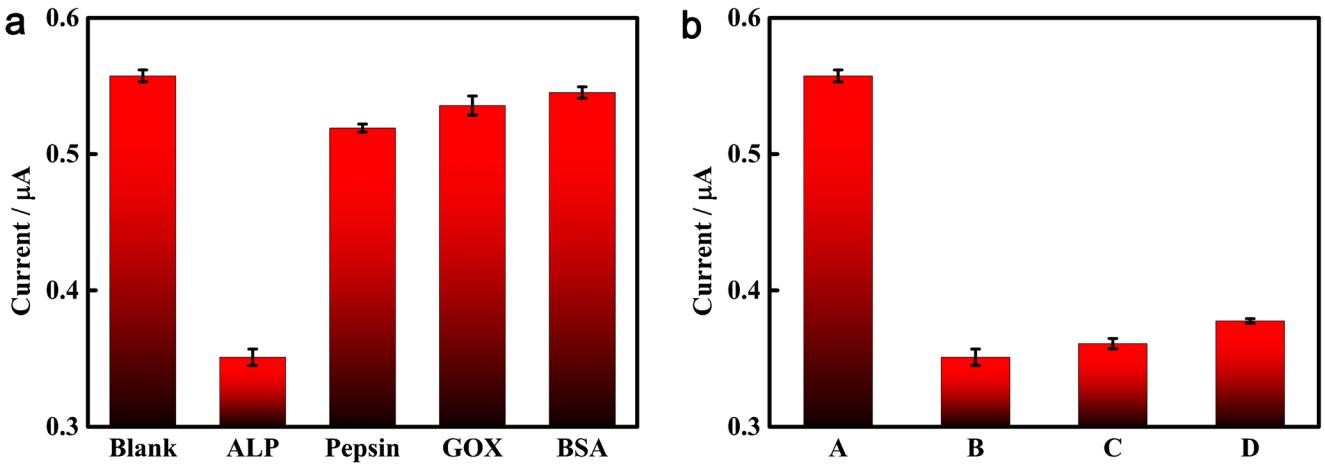

Fig. 7 (a) DPV responses of this biosensor toward without ALP, the ALP (50 mU/mL), pepsin (50 mU/mL), GOx (50 mU/mL), and BSA (100 μM). (b) DPV responses of this biosensor toward without ALP (a), the 50 mU/mL ALP in Tris–HCl buffer (b) and 5% (c) and 10% (d) serum sample. Error bars = SD, $n = 3$

Conclusion

In summary, we have developed an electrochemical biosensor for ALP activity detection based on enzyme-catalyzed reaction and AFC as an electroactive probe. ALP activity detection is realized by using the dephosphorylation property of ALP and one-step conjugation of AFC and phosphoric group, which is easy to operate, time saving, and low cost. Under optimized conditions, the electrochemical biosensor manifests high selectivity and has satisfactory anti-interference capability in serum samples. Therefore, this strategy shows great application prospect as a universal tool for ALP activity determination and inhibitor screening.

Funding This work was supported by the project of tackling of key scientific and technical problems in Henan Province (192102310033); Program for the Key Scientific Research Project of Colleges and Universities in Henan Province (21A360018); and the China Postdoctoral Science Foundation (2016T90669).

Compliance with ethical standards

Conflict of interest The authors declare that there are no conflicts of interest.

References

1. Stenvinkel P. Chronic kidney disease: a public health priority and harbinger of premature cardiovascular disease. J Intern Med. 2010;268(5):456–67.
2. Bikbov B, Purcell CA, Levey AS, Smith M, Abdoli A, Abebe M, et al. Global, regional, and national burden of chronic kidney disease, 1990-2017: a systematic analysis for the Global Burden of Disease Study 2017. Lancet. 2020;395(10225).
3. Go AS, Chertow GM, Fan D. Chronic kidney disease and the risks of death, cardiovascular events, and hospitalization. J Vasc Surg. 2004;41(1):1296–305.
4. Haarhaus M, Brandenburg V, Kalantar-Zadeh K, Stenvinkel P, Magnusson P. Alkaline phosphatase: a novel treatment target for cardiovascular disease in CKD. Nat Rev Nephrol. 2017;13(7):429–42.
5. Ma F, Liu M, Zhang CY. Ligase amplification reaction-catalyzed assembly of a single quantum dot-based nanosensor for sensitive detection of alkaline phosphatase. Chem Commun. 2019;55(61):8963–6.
6. Han YX, Chen J, Li Z, Chen HL, Qiu HD. Recent progress and prospects of alkaline phosphatase biosensor based on fluorescence strategy. Biosens Bioelectron. 2019;148:111811.
7. Zaher DM, El-Gamal MI, Omar HA, Aljareh SN, Al-Shamma SA, Ali AJ, et al. Recent advances with alkaline phosphatase isoenzymes and their inhibitors. Arch Pharm. 2020;353(5).
8. Zhang YY, Li YX, Zhang CY, Zhang QF, Huang XN, Yang MD, et al. Fluorescence turn-on detection of alkaline phosphatase activity based on controlled release of PEI-capped Cu nanoclusters from MnO2 nanosheets. Anal Bioanal Chem. 2017;409(20):4771–8.
9. Song HW, Niu XH, Ye K, Wang LJ, Xu YH, Peng YX. A novel alkaline phosphatase activity sensing strategy combining enhanced peroxidase-mimetic feature of sulfuration-engineered CoOx with electrostatic aggregation. Anal Bioanal Chem. 2020;412(23):5551–61.
10. Zhang LF, Hou T, Li HY, Li F. A highly sensitive homogeneous electrochemical assay for alkaline phosphatase activity based on single molecular beacon-initiated T7 exonuclease-mediated signal amplification. Analyst. 2015;140(12):4030–6.
11. Gwynne L, Sedgwick AC, Gardiner JE, Williams GT, Kim G, Lowe JP, et al. Long wavelength TCF-based fluorescent probe for the detection of alkaline phosphatase in live cells. Front Chem. 2019;7:255.
12. Wang JW, Ni PJ, Chen CX, Jiang YY, Zhang CH, Wang B, et al. Colorimetric determination of the activity of alkaline phosphatase by exploiting the oxidase-like activity of palladium cube@CeO2 core-shell nanoparticles. Mikrochim Acta. 2020;187(2):115.
13. Zhang QF, Zhang CY, Yang MD, Yu DH, Yu C. Pyrophosphate as substrate for alkaline phosphatase activity: a convenient flow-injection chemiluminescence assay. Luminescence. 2017;32(7):1150–6.
14. Hemed NM, Convertino A, Shacham-Diamand Y. Alkaline phosphatase detection using electrochemical impedance of anti-alkaline phosphatase antibody (Ab354) functionalized silicon-nanowire-forest in phosphate buffer solution. Sensors Actuators B Chem. 2018;259:809–15.
15. Hasegawa T, Sugita M, Takatani K, Matsuura H, Umemura T, Haraguchi H. Assay of alkaline phosphatase in salmon egg cell cytoplasm with fluorescence detection of enzymatic activity and zinc detection by ICP-MS in relation to metallomics research. Bull Chem Soc Jpn. 2006;79(8):1211–4.
16. Sun D, Xu WQ, Xu SP. Ultrasensitive Raman sensing of alkaline phosphatase activity in serum based on an enzyme-catalyzed reaction. Anal Methods. 2019;11(28):3501–5.
17. Zhao LY, Yang HX, Zheng XK, Li JG, Jian LH, Feng WS, et al. Dual signal amplification by polysaccharide and eATRP for ultrasensitive detection of CYFRA 21–1 DNA. Biosens Bioelectron. 2019;150:111895.
18. Miao P, Ning LM, Li XX, Shu YQ, Li GX. An electrochemical alkaline phosphatase biosensor fabricated with two DNA probes coupled with λ exonuclease. Biosens Bioelectron. 2011;27(1):178–82.
19. Lee JY, Ahn JK, Park KS, Park HG. An impedimetric determination of alkaline phosphatase activity based on the oxidation reaction mediated by Cu^{2+} bound to poly-thymine DNA. RSC Adv. 2018;8(20):11241–6.
20. Miao XM, Guo XT, Xiao ZY, Ling LS. Electrochemical molecular beacon biosensor for sequence-specific recognition of double-stranded DNA. Biosens Bioelectron. 2014;59:54–7.
21. Wei W, Ni QW, Pu YP, Yin LH, Liu SQ. Electrochemical biosensor for DNA damage detection based on exonuclease III digestions. J Electroanal Chem. 2014;714:25–9.
22. Hu Q, Deng XB, Kong JM, Dong YY, Liu QR, Zhang XJ. Simple and fast electrochemical detection of sequence-specific DNA via click chemistry-mediated labeling of hairpin DNA probes with ethynylferrocene. Analyst. 2015;140(12):4154–61.
23. Hu Q, Deng XB, Yu XH, Kong JM, Zhang XJ. One-step conjugation of AFC to phosphate groups as electroactive probes for electrochemical detection of sequence-specific DNA. Biosens Bioelectron. 2015;65:71–7.
24. Ghosh SS, Kao PM, McCue AW, Chappelle HL. Use of maleimide-thiol coupling chemistry for efficient syntheses of oligonucleotide-enzyme conjugate hybridization probes. Bioconjug Chem. 1990;1(1):71.
25. Tang ZW, Chen HT, He HL, Ma CB. Assays for alkaline phosphatase activity: progress and prospects. Trends Anal Chem. 2019;113:32–43.
26. Hu Q, Wang QW, Sun GZ, Kong JM, Zhang XJ. Electrochemically mediated surface-initiated de novo growth of polymers for

amplified electrochemical detection of DNA. Anal Chem. 2017;89(17):9253–9.
27. Zheng XK, Liu QR, Li MM, Feng WS, Yang HX, Kong JM. Dual atom transfer radical polymerization for ultrasensitive electrochemical DNA detection. Bioelectrochemistry. 2020;133.
28. Wang T, Zhang Z, Li YY, Xie GM. Amplified electrochemical detection of mecA gene in methicillin-resistant Staphylococcus aureus based on target recycling amplification and isothermal strand-displacement polymerization reaction. Sensors Actuators B Chem. 2015;221:148–54.
29. Hu Q, Han DX, Gan SY, Bao Y, Niu L. Surface-initiated-reversible-addition-fragmentation-chain-transfer polymerization for electrochemical DNA biosensor. Anal Chem. 2018;90:12207–13.
30. Ni JC, Wang QX, Yang WQ, Zhao MM, Zhang Y, Guo LH, et al. Immobilization free electrochemical biosensor for folate receptor in cancer cells based on terminal protection. Biosens Bioelectron. 2016;86:496–501.
31. Cheng D, Zhang YP, Wen DX, Guo ZZ, Yang HX, Liu YJ, et al. Hairpin probes based click polymerization for label-free electrochemical detection of human T-lymphotropic virus types II. Anal Chim Acta. 2019;1059:86–93.
32. Deng JJ, Yu P, Wang YX, Mao LQ. Real-time ratiometric fluorescent assay for alkaline phosphatase activity with stimulus responsive infinite coordination polymer vanoparticles. Anal Chem. 2015;87(5):3080–6.
33. Lu ZX, Wu JS, Liu WM, Zhang YY, Wang PF. A ratiometric fluorescent probe for quantification of alkaline phosphatase in living cells. RSC Adv. 2016:32046–51.
34. Li CM, Zhen SJ, Wang J, Li YF, Huang CZ. A gold nanoparticles-based colorimetric assay for alkaline phosphatase detection with tunable dynamic range. Biosens Bioelectron. 2013;43:366–71.
35. Jiang H, Wang XM. Alkaline phosphatase-responsive anodic electrochemiluminescence of CdSe nanoparticles. Anal Chem. 2012;84(16):6986–93.
36. Akhtar H, Silvana A. Nanoceria particles as catalytic amplifiers for alkaline phosphatase assays. Anal Chem. 2013;85(21):10028–32.